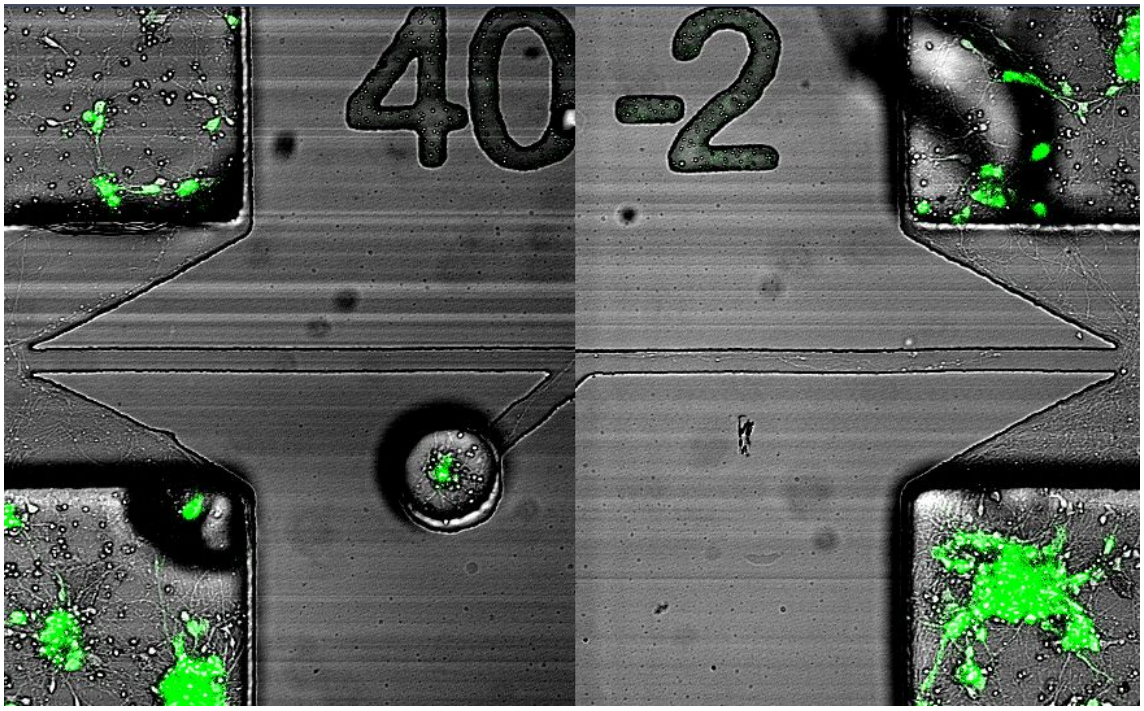

Geometrical Axon Guidance

with PDMS Microstructures

Master's Thesis in Applied Physics - TIFX03

Sandra Ines Speicher

Department of Applied Physics
CHALMERS UNIVERSITY OF TECHNOLOGY
EIDGENOESSISCHE TECHNISCHE HOCHSCHULE ZÜRICH
Gothenburg, Sweden 2015

Geometrical Axon Guidance with PDMS Microstructures

Sandra Ines Speicher

Department of Applied Physics
CHALMERS UNIVERSITY OF TECHNOLOGY
EIDGENOESSISCHE TECHNISCHE HOCHSCHULE ZÜRICH
Gothenburg, Sweden 2015

Geometrical Axon Guidance with PDMS Microstructures
Sandra Ines Speicher

©Sandra Ines Speicher, 2015.

Department of Applied Physics
Chalmers University of Technology
SE-412 96 Gothenburg
Sweden

Cover:
The title page shows a confocal laser scanning microscope image of a PDMS micro-structure in form of an 120°-to-40° T-junction 7 days post-seeding with primary coritcal rat neurons, which have been transfected with a viral vector making them produce green fluorescent protein. The processes of the neurons in the central well have exclusively extended into the obtuse channel.

Department of Applied Physics
Gothenburg, Sweden 2015

Abstract

Having circuits made of single neurons would bring us a big step closer to a full understanding of the neuronal system. To build these networks and more, we need to find a way to guide axons in specific directions. Learning about their turning behavior in predefined geometric environments was the scope of this project. In order to enable a statistical analysis of the axons' behaviors in geometrically defined environments, microstructures with repetitive patterns of T-junction channels were designed in AutoCAD and fabricated in polydimethylsiloxane (PDMS) from SU8 molds that had been made using photolithography. The design of the T-junctions was varied in different parameters such as the angle of incident of the upstroke of the 'T' against the horizontal stroke or the relocation of the upstroke closer towards one side of the horizontal stroke. These structures were stuck onto laminin or poly-D-lysine (PDL) coated WillCo dishes and seeded with primary cortical rat neurons. The neurons were transfected with a viral vector to enable fluorescence imaging with a confocal laser scanning microscope (CLSM).The time frame of the project did not allow for the performance of a statistical analysis, but important milestones were set for the preparation thereof. Structure designs that aid an automatized imaging process were found, the fragile culturing conditions primary neurons need to stay alive and grow axons were met and the automatization of the imaging itself was successfully implemented. A trend in the axon bending behavior was recognized.

Keywords: axon bending, neuronal networks, geometrical guidance, PDMS, microstructures, PDL, laminin

Contents

1 Introduction **1**

2 Aim **2**

3 Background **3**
3.1 Neurons . . . 3
3.2 Previous Research . . . 3
3.2.1 Neurons in 3D Geometries . . . 3
3.2.2 Turning Ability of Axons . . . 4
3.2.3 Axon Turning versus Branching . . . 4
3.3 Theory of Methods . . . 4
3.3.1 Photolithography . . . 4
3.3.2 Confocal Laser Scanning Microscopy . . . 5
3.3.3 Viral Transfection . . . 5

4 Materials and Methods **7**
4.1 Fabrication of PDMS Microstructures . . . 7
4.1.1 Mask Design . . . 7
4.1.2 Mold Microfabrication . . . 7
4.1.3 PDMS Casting . . . 8
4.1.4 Sample preparation . . . 8
4.2 Neuron Culture . . . 8
4.3 Axon Imaging and Analysis . . . 8

5 Results **10**
5.1 Microstructure Designs . . . 10
5.1.1 Mask M3 . . . 10
5.1.2 Mask M4 . . . 10
5.1.3 Mask M5 . . . 10
5.1.4 Mask M6 . . . 10
5.2 Microstructure Examination . . . 12
5.3 Neuron Culture Monitoring . . . 12
5.4 CLSM Axon Imaging . . . 13
5.4.1 CLSM Images . . . 13
5.4.2 Axon Turning Counts . . . 15

6 Discussion **17**
6.1 Mask Design . . . 17
6.2 Culturing Conditions . . . 17
6.3 Imaging Technique . . . 17
6.4 Axon Turning Behavior . . . 18

7 Suggestions for Further Experiments and Analysis **19**

8 Conclusion **20**

9 Acknowledgements **21**

References **22**

Appendix: CLSM Automatization Protocol

1 Introduction

There is a reason, why the brain is one of the most exciting fields of research of the 21st century. The topics neuroscience traverses are vastly interesting. Treatment of mental diseases, controlling bionic limbs, understanding data storage in humans and applying this knowledge to possibly even download or upload information from the brain or use the brain's unique capabilities for image processing or as a model for the development of artificial intelligence are just a few examples of a huge variety.
With all the possible benefits in mind it should come as no surprise, that the approaches for making progress in these important areas are just as diverse. From microscoping brain slices or performing behavioral experiments to looking into the brains of living beings with Magnet Resonance Imaging and large-scale in-vivo electrical recordings, researchers keep on introducing new methods to learn more about the subject.
Their is a big issue with irreproducible data though. In order to allow for a precise, non-statistical analysis of the fundamental dynamics of neural networks, we are working on culturing them in-vitro. This way we gain greater control over the networks' surrounding conditions which should lead to higher reproducibility of the findings. From investigating networks comprising of small numbers of neurons we gain understanding and then want to gradually increase the complexity of the systems.
For constructing a network of neurons, we need to be able to on the one hand place individual neurons at predefined spots and on the other hand guide their axons to make specific connections between the neurons. The latter seems especially important and has been neglected in the previous research which is why we chose it as the focus of this project. More precisely we look at the direction of growth of the axons in specified environments. Their behavior at T-crossings with various angles of incidence could give us crucial information on e.g. how to construct pathways that force neurons to connect in a directed net.

2 Aim

The aim of this project is to explore the bending behavior of axons in micro-fabricated T-junctions with precisely engineered crossing angles under the hypothesis that axons are most likely to bend away from obstacles in the smallest possible angle to avoid bending sharper than necessary.

3 Background

The following section provides information useful for understanding the further content of this report. Basic knowledge about neurons is presented first, then a brief summary of the previous research in the field and last is background information about some of the more sophisticated methods used.

3.1 Neurons

Being able to identify neurons under the microscope is an essential part of this work which is why an understanding of their morphology is helpful. In Figure 1, the typical shape of several neurons' cell bodies and the processes growing out of them are clearly visible. Brains are composed to only about 1/4 of neurons and to 3/4 of glial cells [1], a homogeneous neuron culture can be maintained with the right medium.
Other useful information to consider when designing experiments that include growing axons is their growth speed which can reach 1mm/day [2]. In previous experiments with our cells (primary rat cortex, for further specification see Section 4.2) it has been observed to be more in the range of 0.1mm/day though. Substrates that axons seem to grow well on are laminin [3] and poly-lysine [4, 5].

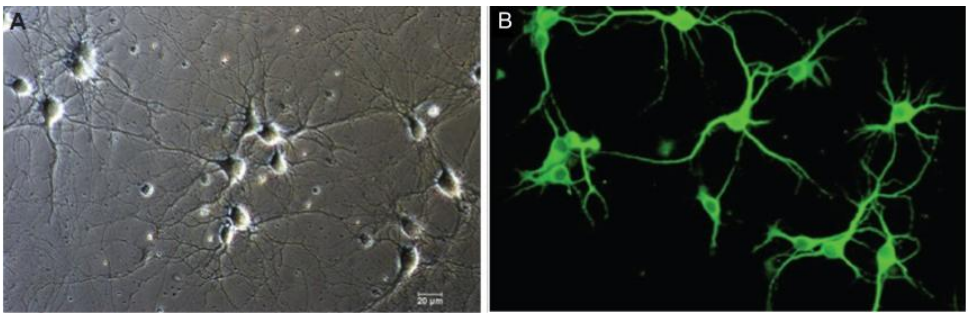

Figure 1: Typical neuron morphology under a phase contrast (A) and fluorescence (B) microscope. [6]

3.2 Previous Research

There have been few publications prior to this work, which deal with related topics like integration of topographical cues, bending ability of axons and pathfinding models. Useful information extracted from their findings is summarized in the following paragraphs.

3.2.1 Neurons in 3D Geometries

In 2007, Li and Folch [7] examined the behavior of cortical neurons in 3D geometries focusing on whether axons would integrate biochemical and topographical cues. Therefore they micro-fabricated polydimethylsiloxane (PDMS) steps of different sizes and coated them with poly-D-lysine (PDL). One observation they made was that axons growing towards these steps facing either a vertical wall or edge from a certain step height on

($\tilde{}10 - 11\mu$m) would almost always choose the smallest possible turning angle, making the general assumption that axons prefer to minimize their bending angle.

3.2.2 Turning Ability of Axons

Francisco et al. [8] tested the ability of ganglial neurons to grow their axons around corners in laminin coated silicon-SU8 corridors. They found that the amount of axons turning around a corner can be increased by widening the corridors and choosing softer corner angles. It was proven that angles as sharp as 45° are no problem for the axons to turn around.

3.2.3 Axon Turning versus Branching

The findings by Francisco et al. described in the previous section were used for a neurotoxicity test by Wei et al. in 2014 [9]. They seeded single cortical neurons in T- or Y-patterns made of PDMS with a PLL-L1-coating and monitored the influence of the exposure to a neurotoxin on the axons' turning and branching behaviour. In this single-neuronaxonal pathfinding model a microchannel depth and width of 20μm and a microwell diameter of 50μm was found to be most beneficial in measures of the polarity and viability of the neurons.

3.3 Theory of Methods

The most important methods used during this project were photolithography for providing the geometrical structures the neurons were cultured in and viral transfection to make them fluorescent for the CLSM imaging. To give a better insight into the performed work, the theory of these methods is provided here.

3.3.1 Photolithography

The working principle of photolithography is visualized in Figure 2. A substrate is coated with a substance called photoresist. A mask is placed on top of the coating to shield predefined areas from the UV light, which is then applied to cross-link the photoresist. Only the shielded photoresist regions can be removed with developer later on. The method is popular for its simplicity and reproducibility.

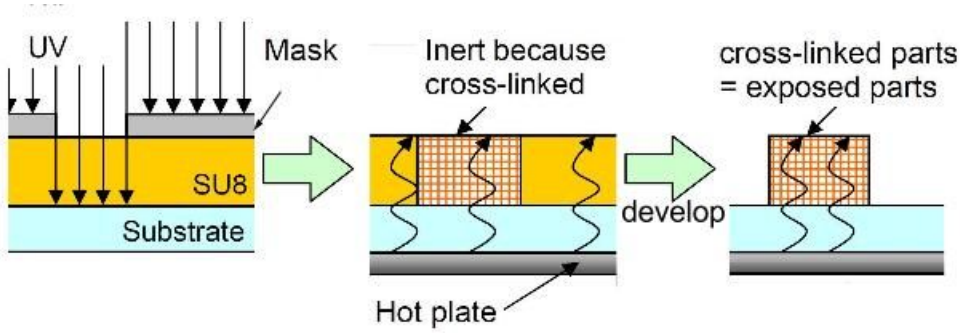

Figure 2: Scheme of a photolithography process. A photorestist (here SU8) is covered by a partially transparent mask. The regions that get exposed to UV light are cross-linked. Developing leaves only these parts on the substrate. [10]

3.3.2 Confocal Laser Scanning Microscopy

A Confocal Laser Scanning Microscope (CLSM) is a fluorescence microscope. Fluorescence microscopy is commonly used in bio related fields because it enables distinguishing specific structures or cells in a sample. If the target is not fluorescent by itself, it gets stained with a respective dye. An incoming light beam of the right wavelength is used to excite the sample, see Figure 3. Fluorescence occurs by emission of lower energy light during the relaxation of the excited atoms. By installing a suitable filter, only the fluorescent structures get detected and processed into an image.
CLSMs have a special feature which enables isolated imaging of focal planes in variable z-depth of the sample. This is achieved by installing a pinhole in the specific focal plane on the ocular side which resembles exactly the one specimen focal plane one wants to observe thus blending out most of the light coming from the other specimen focal planes.

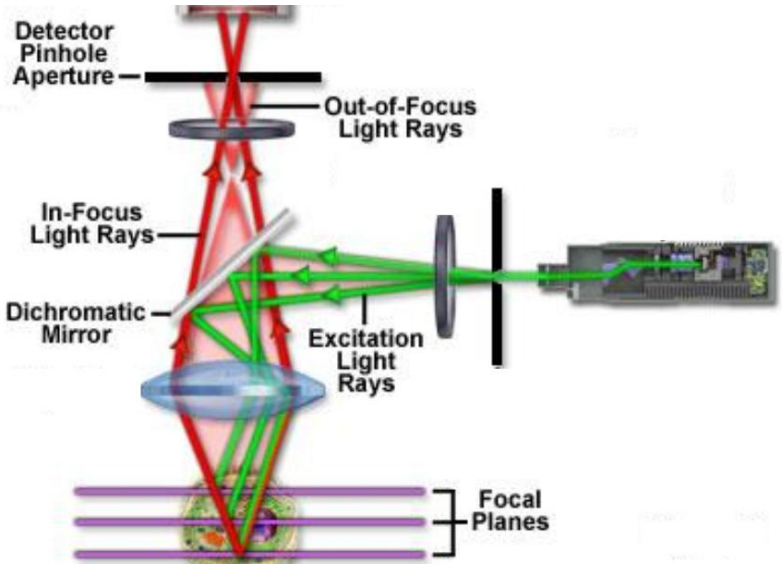

Figure 3: Scheme of a confocal laser scanning microscope. The excitation light rays get reflected by a dichromatic mirror and excite different focal planes in the specimen. The fluorescence passes the mirror but a pinhole aperture is placed in front of the detector shielding most of the intensity of the out-of-focus light rays. Only in-focus light rays get through with full intensity, an image of one single focal plane gets detected. [11]

3.3.3 Viral Transfection

Even though regular cell trackers are becoming better and better, toxicity and the limited substance volume that can practically be applied to a sample are still an issue [12]. Latter is especially true for long term imaging since the tracker intensity will fade. The limitation is also inconvenient in setups like our passive channel systems in which the distribution of the substance can not be facilitated with pumps and thus depends strongly on diffusion. Viral transfection is a technique which uses a virus to deliver a piece of RNA (ribonucleic acid) into a cell, see Figure 4. The incorporated RNA will then be translated as if it was

the cell's own RNA creating a theoretically endless source of the respective protein and solving the issues of limited substance volume. The RNA piece can be engineered to be translated into any protein, for fluorescent imaging purposes GFP (green fluorescent protein) is a popular one.

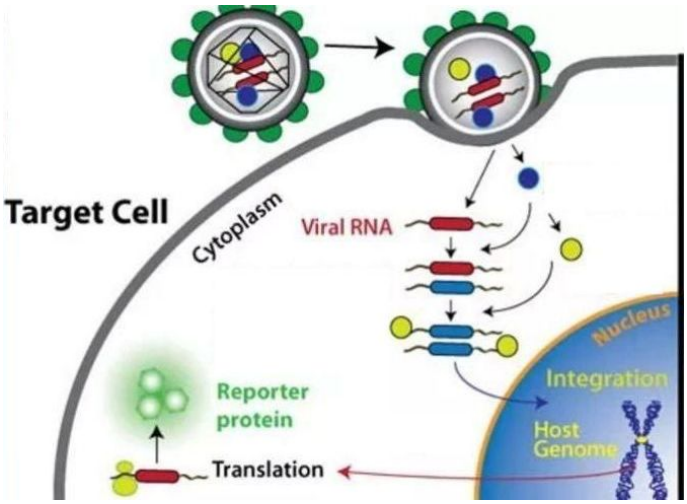

Figure 4: Scheme of a viral transfection. A virus is brought into the direct surrounding of the target cell. It introduces i.a. RNA into the cytoplasm. After a series of steps, the sequence gets integrated into the host genome. It is translated and a (reporter) protein is produced. [13]

4 Materials and Methods

A number of steps were fulfilled in order to achieve the aim of the project: Microstructures were tailor made from PDMS, neurons were cultured in these geometric environments and finally the growth direction of their axons was analyzed.

4.1 Fabrication of PDMS Microstructures

The microstructures were created by casting PDMS into photolithographically produced molds on silicon wafers.

4.1.1 Mask Design

The design of the microstructures was drawn in Autodesk AutoCAD 2015.
The basic idea was to create T-shaped channels as depicted in Figure 5 so that a neuron sitting in a microwell at the lower end of the 'T' would grow its axon towards the crossing where it has the choice to turn either left or right. To support the culture two bigger microwells were implemented at both sides of the 'T'. Their width was chosen $20\mu m$ in compliance with Wei et al. [9].
This basic layout was then modified to check the axons behavior for different colliding angles of the upstroke of the 'T' with its crossbar, varied lengths of the two sides of the crossbar and altered well sizes. Columns of different T-designs were reproduced in identical rows to enable statistical evaluation.
For the photolithography, three layers of masks were used: One with the complete design, one with towers representing the openings of the microwells and one more with a pattern for alignment which has to be incorporated in the other two layers as well.

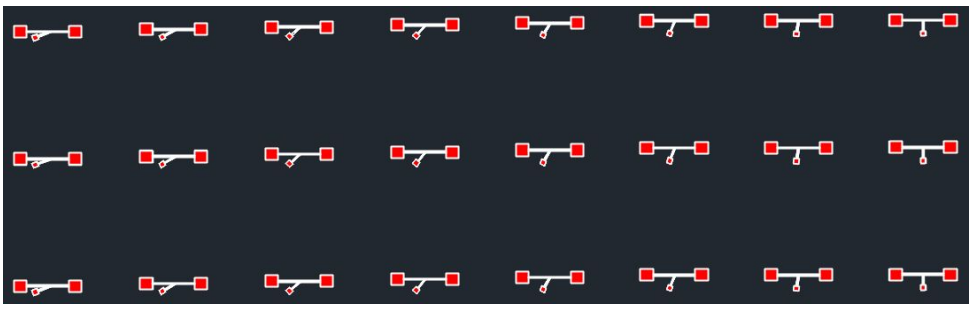

Figure 5: Basic design of the lithography masks. White represents the ground layer mask for the T-shaped channels. Red represents the upper layer mask for the microwells. Scale: One structure is 1.32mm wide from left to right.

4.1.2 Mold Microfabrication

The mold fabrication was performed by photolithography on clean silicon wafers. First, the wafers were marked with the alignment pattern by following the lift-off protocol of micro resist's ma-N 1410 photoresist [14] in combination with gold sputtering. Second, the negative of the complete channel and microwell-design was lithographed in a $10\mu m$

SU-8 layer of Gersteltec GM 1060 according to the official protocol [10]. This height was chosen for the channels in an effort to allow only the axons and not entire cell bodies to enter them. Third, $300\mu m$ high towers representing the holes of the microwells were created in a second layer of SU-8 (Gersteltec GM 1075) [15].
The molds were imaged with a microscope for quality check.

4.1.3 PDMS Casting

After rendering the wafers anti-adhesive with fluorinated silanes the molds were spin-coated with degassed PDMS ($1 : 10$ cross-linker : PDMS). Prepared PDMS rectangles were attached around the outlines of the microstructure arrays for stabilization during the removal of the PDMS sheets. The structures were baked for four hours at $> 80°C$.
A quality check was performed by sputtering a part of the PDMS sheet with gold, which enabled clear identification of open wells under a microscope.

4.1.4 Sample preparation

The PDMS structures were sterilized by immersing them in 100% ethanol overnight.
The substrates (WillCo-Dish GWSB-5040) were wiped with 10% Rush and plasma-cleaned. They were coated with either PDL (Sigma-Aldrich) or laminin (Sigma-Aldrich) for better cell adhesion.
To close the channels, the PDMS sheets were attached to the substrates with the open side of the channels facing the glass. Monahan et al.'s Channel Outgas Technique [16] was used to fill the microchannels with culture medium pre-seeding.

4.2 Neuron Culture

Primary rat neurons from freshly dissected embryonic rat cortices (day 9) were seeded into the microstructures at a concentration of $200.000 cells/cm^2$. They were kept in an incubator and fed with neurobasal medium twice a week.
The viability and rough status of the axon formation of the neurons was spot-checked with a contrasting microscope.
In order to enable fluorescence imaging, the neurons were transfected with a virus (Penn Vector Core AAV9.Syn.GCaMP6s.WPRE.SV40) to make them produce GFP.

4.3 Axon Imaging and Analysis

The axons were imaged with a CLSM (Carl Zeiss AG/LSM 510). The software (Zen2009) was used to create an automatization protocol for faster imaging of the large number of regularly arranged microwells. For detailed protocol see 'Appendix: CLSM Automatization Protocol'. The analysis was performed by manually browsing through the images with Carl Zeiss ZEN 2.1 (black, Version 11,0,0,190) in Image Processing mode and linking the observations to specific properties of the specimens. The turning behavior of the axons in the different microstructures was registered in a chart to see a possible correlation. This was done in an all-or-nothing manner since it was not possible to count the number of axons in the tangles and because the first axon that had turned the corner may have induced turning in the same direction in the others. For samples in which axons

turning in both directions appeared a point was added for each of the directions in the chart.

5 Results

Results of the experimentation include the microstructure designs that were drawn from the examinations of the fabricates. Regarding the neurons, there are results from the monitoring of the cultures themselves and the images of the axons and their analysis.

5.1 Microstructure Designs

The basic layout was modified in various ways to increase the traceability of the experiments and simplify automated imaging. Also, different designs were created in an effort to enable examination of the bending statistics of axons not only in dependence of the angle but also of the proximity and/or amount of neighbor neurons.

5.1.1 Mask M3

Each microstructure was labeled with the angle of the T-crossing and the number of the row for better tracking, see Figure 6 a. Angles were varied in steps of 10° from 20° to 90°. In total, 9 identical rows fit onto one WillCo-Dish.

5.1.2 Mask M4

In mask M4 (see Figure 6 b), other incentives than the angle were altered. In the first four columns (A-D), that was the distance of the upstroke of the 'T' to the side wells as opposed to the middle position it had been situated in before. In the last four columns (E-H), the same was repeated but with the closer side well reduced to a size of 0.1x0.1mm in order to allow less supporting neurons to settle there during the experiments.

5.1.3 Mask M5

As apparent from Figure 6 c, a new basic design was proposed for mask M5. The side wells were redesigned with the goal to make it harder for axons from the supporting cultures to grow into the channel. They were also duplicated to make them double in size. The channel of the upstroke of the 'T' was shortened to 0.15mm so that the axon from the now round shaped experimental well would grow to the point of interest faster.

5.1.4 Mask M6

Mask M6 (see Figure 6 d) resembles a translation of M4 into the basic design of M5 with the minor change that only two different distances were compared to the middle position. In addition, the size of the side wells was varied from full to a half and to a quarter.

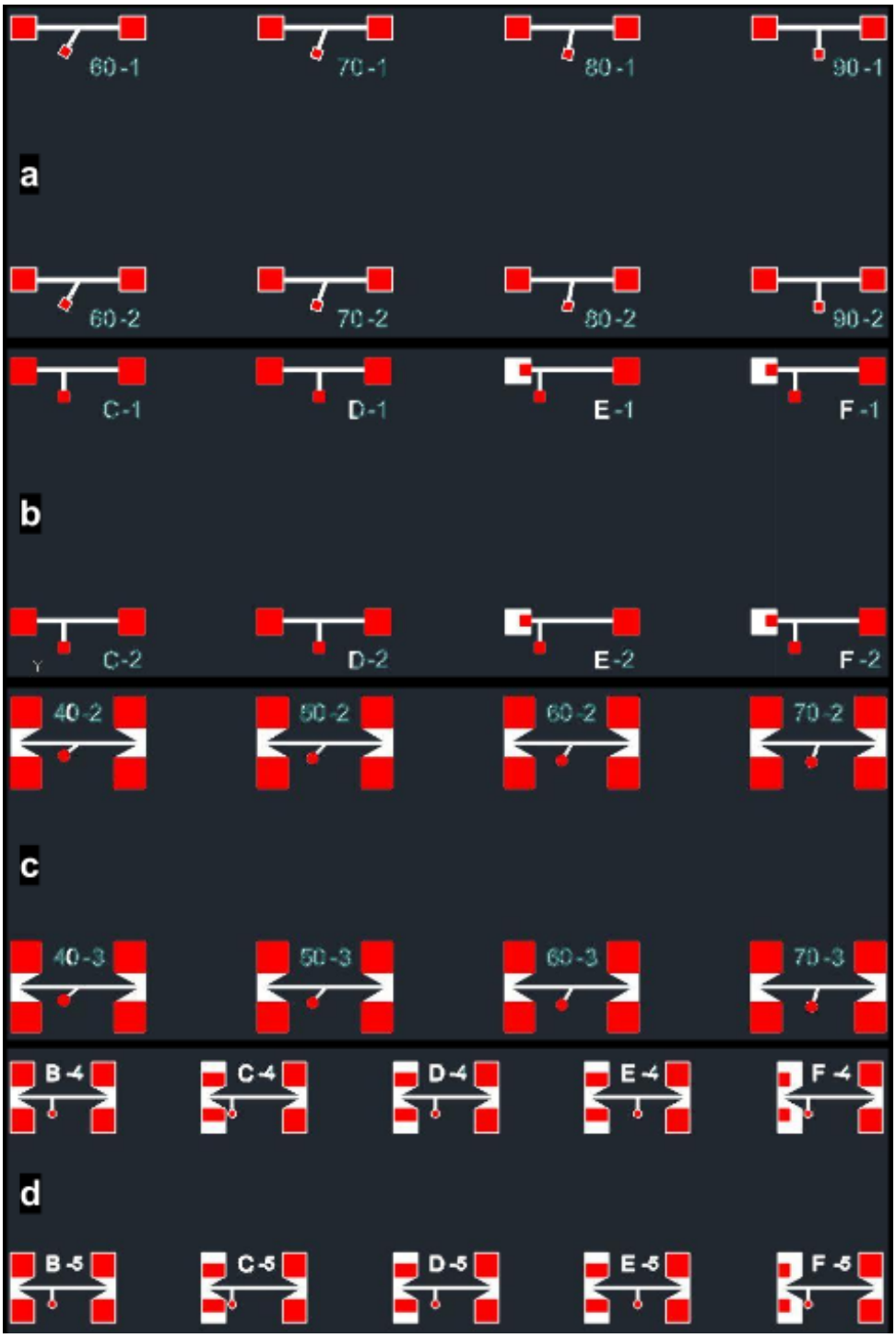

Figure 6: Top-view of masks M3 (a), M4 (b), M5 (c) and M6 (d) in AutoCAD. White represents channels, red wells and the numbers 'column'-'row'. Scale: One structure is 1.32mm wide from left to right.

5.2 Microstructure Examination

Microscope images of the mold as exemplified in Figure 7 A showed mainly intact SU8-structures on the silicon wafers. Also, after removing the PDMS foils from the molds most of the 'towers' looked as if they had PDMS residues left on top of them which would mean the microwells had been pinched open in the PDMS.
This was confirmed by a large part of the images that were taken of the gold-sputtered PDMS foil samples. As visible in Figure 7 B, the microwells are indeed mostly open, while the channel is covered.

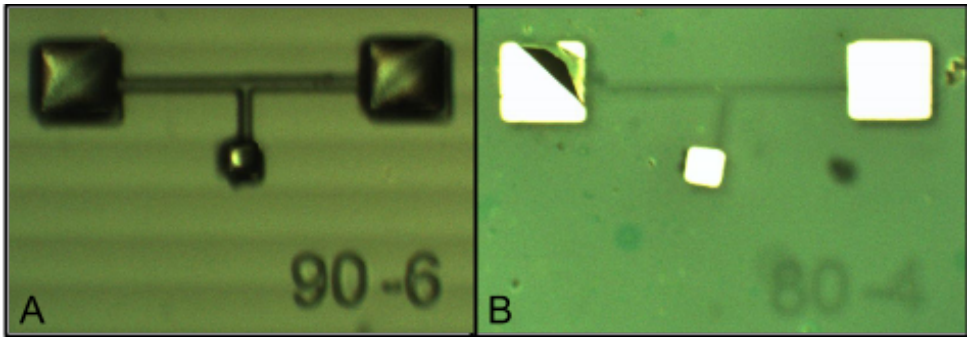

Figure 7: Sample microscope images of a microstructure on the wafer after PMDS peel off (A) and a microstructure in PDMS after sputtering (B). Scale: One structure is approximately 1.32mm wide from left to right.

5.3 Neuron Culture Monitoring

Under the contrast microscope a lot of seeded microstructures were visible as exemplified in Figure 8. The cells are more spread out on PDL (see 8 B). Laminin adheres less strongly onto the substrate which made formation of clusters more likely(see Figure 8 A). On the PDL coated substrates, there are regions visible which could be PDMS debris or dead cells. Axon growth was observed on both coatings.

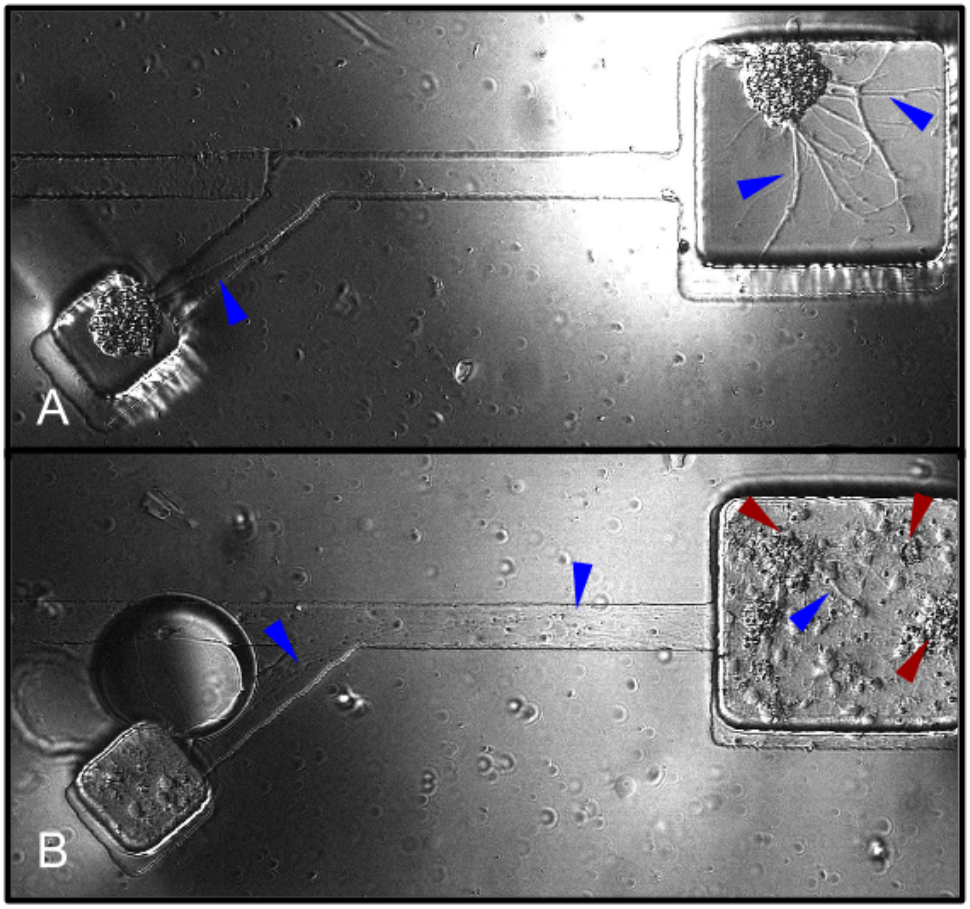

Figure 8: Sample contrast microscope images of M3 PDMS structures on (A) laminin- and (B) PDL-coated WillCos on day 7 after seeding with neurons. Red arrows may indicate PDMS debris or dead cells, blue arrows indicate axons. Scale: The horizontal channel is approximately 0.02mm wide from bottom to top.

5.4 CLSM Axon Imaging

The automated CLSM imaging method delivered complete image catalogs of the dishes. These enable more detailed observations than the sample images from the contrast microscope. Axon turning was captured for three of the dishes. Tables illustrate the findings from the manual evaluation of the turning behavior.

5.4.1 CLSM Images

Some of the most interesting observations from the CLSM image catalog are exemplified in Figure 9. In part A, a single axon grows out of the central microwell into the channel and takes a turn around the obtuse angle. At the same time, the axons stretching out from the supportive microwells are still confined in their especially shaped double-triangular spaces.
Similar behavior can be observed in Figure 9 B. Here, the supportive cultures have also grown a lot of axons that have not entered the channel. The neurons in the experimental well on the other hand have formed multiple tangled up axons. They appear to separate at the corner of the T-crossing, bending in both directions.

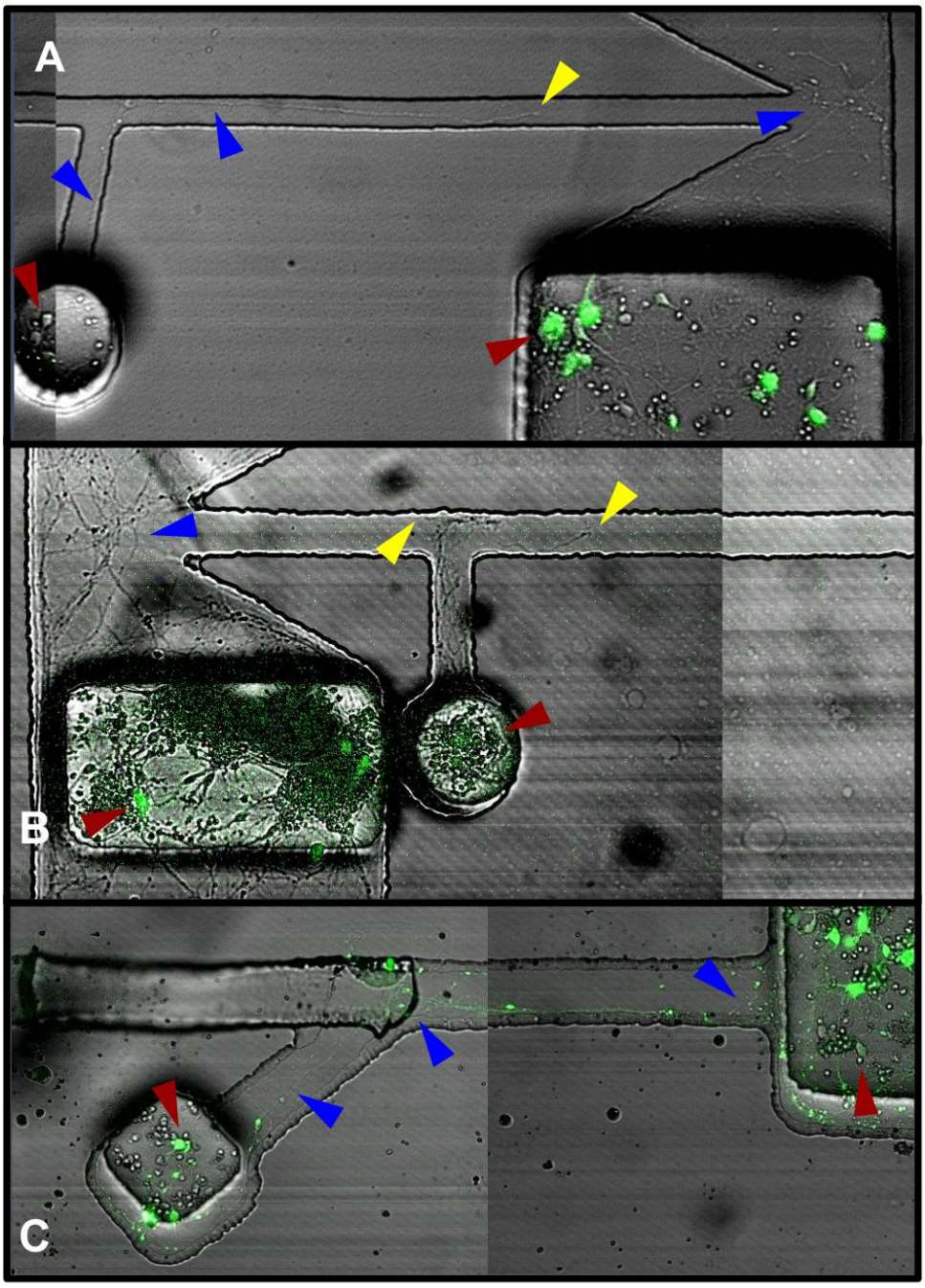

Figure 9: CLSM image details of (A) a M5-80°-, (B) a M6-C- and (C) a M3-40°-microstructure 7 days post seeding and 6 days post transfection. The images are overlays of a fluorescence (green) and the transmission channel (grayscale). Red arrows indicate cells, blue arrows axons and yellow arrows axon tips. Scale: The horizontal channels are approximately 0.02mm wide from bottom to top.

In contrast to the first two images, part C shows a different situation. Axons expand throughout the whole length of the channel making it impossible to tell whether they grew out of the central or the side well. So even if there was no SU8-residue stuck inside

the channel one could not draw a conclusion about the turning behavior of the axons from this image.
These two problems each appeared in more than half of the microstructures in M3- and M4-samples, sometimes individually sometimes combined, but in less than 10% of the microstructures in the M5-and M6-samples. On the other hand, there appeared to be around twice as many malformations in the PDMS molds of those more complex structures, especially in the M5-20°-microstructures.
Other interesting observations include that while the cells did well on five of the six PDL-coated dishes, axon-growth was not observed in any of the laminin-coated dishes in the CLSM. It should also be mentioned that in some cases neurons did enter the channels with their complete cell bodies. And that the transfection did not result in sufficient fluorescence within a reasonable time frame, as also visible in Figure 9.

5.4.2 Axon Turning Counts

Because of the aforementioned problems only three of the samples (one M3-, one M5- and M6-dish, all with PDL-coating) added to the axon turning counts. The numbers are too small to perform a statistical analysis on them but Figure 10 displays a tendency for the axons to bend around the more obtuse angle that seems to get stronger the more obtuse the angle gets.

	20	30	40	50	60	70	80	90
O(M3-PDL)	0	1	0	0	1	0	0	2
A(M3-PDL)	0	0	0	1	1	0	0	2
O(M5-PDL)	2	6	5	5	4	5	6	2
A(M5-PDL)	1	0	2	1	2	4	4	2
ΣO	**2**	**7**	**5**	**5**	**5**	**5**	**6**	**4**
ΣA	**1**	**0**	**2**	**2**	**3**	**4**	**4**	**4**
ΣO - ΣA	**1**	**7**	**3**	**3**	**2**	**1**	**2**	**0**

Figure 10: Counts of microstructures (20-90) in which axon bending towards the obtuse (O) or acute (A) side of the angle of incidence occured in one M3 and one M5 sample with PDL coating, the sums of the obtuse and the acute turning counts and their difference.

It is even more difficult to make a deduction from the numbers presented in Figure 11 since the difference between the axons turning left or right is negligible when looking at each microstructure shape individually. When looking at them collectively though there appears to be a tendency to turn to the right side which was designed to have supportive microwells that are further away from the central well but bigger.

	A	B	C	D	E	F	G	H
L(M6-PDL)	0	3	1	1	2	1	3	0
R(M6-PDL)	0	2	4	3	3	3	2	0
L - R	0	1	-3	-2	-1	-2	1	0

Figure 11: Counts of microstructures (A-H) in which axon bending towards the left (L) or right (R) side occured in an M6 sample with PDL coating and their difference.

6 Discussion

Interesting observations were made about the old versus the new mask design, the culturing conditions and the imaging technique. Even though the axon turning behavior could not be correlated to the crossing angle with statical significance, it is still worth taking a closer look at.

6.1 Mask Design

The different mask designs showed some clear pros and cons. The new basic design of mask M5 and M6 brought a definite advantage in terms of much less unwanted axons from the side wells growing into the channel. On the other hand, the partially very thin walls, e.g. in the 20°-microwells, were not practicable for the else satisfying fabrication method. Still, the new basic design contributed a lot more to the results.
Numbering the structures was obviously very useful for the traceability. A disappointment came with using the channel dimensions referenced in the previous research [9] as a number of neurons were able to enter the channel, fortunately that did not have a great influence on the outcomes this time.
It is not clear whether the reduced incidents of residue stuck in the channel is due to the new mask design being more supportive of the structure or simply because of the progressive mastery of the fabrication process.

6.2 Culturing Conditions

The conflicting interests of having an as small as possible number of neurons in the experimental well and not crowding the transmission images too much but still having enough neurons to support the culture were balanced pretty well under the compromise of a cell density of $0.2 mio/cm^2$.
When it comes to the coating of the WillCo dishes, the CLSM images revealed a definite advantage of PDL over laminin since there simply were no axons in the laminin-dishes.

6.3 Imaging Technique

As far as the imaging technique is concerned, the main topic of discussion of the project is fluorescence versus transmission. The z-resolution of the confocal microscope theoretically is a huge advantage for our layered samples with neurons from up on the top of the PDMS possibly causing disturbances in the images of the ground layer neurons down in the wells and especially the axons in the channels. With the type of CLSM we used the z-resolution works only for the reflected fluorescence. Unfortunately, to achieve an adequate image quality, the acquisition time has to be set 8x longer than what was possible for our regular automatized imaging protocol, which lead to low intensities in the fluorescence image. The low cell densities further benefited the quality the transmission images arguably even making them the better choice.

6.4 Axon Turning Behavior

With less than 100 out of a couple thousand CLSM images displaying the turn of an axon from the experimental well, a significant statement about the turning probability of axons in correlation to the geometry of the environment can not be made at this point. However, there seems to be a preference of the axons to bend around the more obtuse angle which gets stronger the higher the difference between the angles, e.g. 30° versus 150°. This would fit the expectation and could be accounted for by the hypothesis that it is easier for the axons to bend around more angles the more obtuse they are.
The tendency of the axons to prefer bending towards the bigger over the closer supportive well was even slighter. In case of statistically relevant reproduction of the result, this could mean that the quantity of neighboring neurons is a stronger incentive for the growth direction choice of axons than their proximity, at least in the very confined spaces that were looked at during this project.

7 Suggestions for Further Experiments and Analysis

There are a number of further experiments and analysis techniques that did not fit into the time frame of this thesis work but could be helpful for possible subsequent projects:
The mask design should be reworked slightly in order to erase the problem of too thin walls and smaller channel widths should be tested.
Another suggestion, that might be rewarding in respect of time efficiency for large numbers of images, would be the development of an algorithm for computational image analysis which automatically gives out the information whether the axon is turning left or right. To enable this, some other methods would need to be improved first though.
For instance, further optimization towards having single neurons in the experimental wells would probably make the implementation of the algorithm a lot easier because there would not be multiple axons growing out of one experimental well. Furthermore, optimizing the image quality in terms of acuity, resolution and contrast could increase the likelihood of a computational image analysis to be successful.
In context with that, optimization of the (timing of the) viral transfection to possibly get a higher intensity of the fluorescence and therefore better confocal images and better detectability of the axons is another suggestion. Otherwise, one could also consider using a transmission CLSM to get the benefit of the confocal z-resolution also for the transmission image and thereby eliminate problems with the fluorescence which also includes long delivery times and the monetary cost of the virus.

8 Conclusion

The outcome of the project is substantial. Important milestones were reached by achieving the fragile culturing conditions and the new basic design of the micro structures as well as the complete image catalogs with the automatized imaging protocol. First of which is especially difficult when wanting to work not only with primary neuron but their axons. The second point almost eradicated the problem of the axons from the side wells growing into the channel which had been a big problem before since they had been impossible to distinguish from the ones from the experimental well. Also the third was very significant, because imaging all the wells by hand would take too much time when aiming for a number high enough for a statistical analysis.
So, even though the goal of analyzing the bending behavior of neurons in taylor-made structures and with an also taylor-made analysis method was set rather high for the restricted time frame of the project - especially when taking the difficulty of working with the axons of primary neurons into account - the aim was almost fully met and fulfilling the remaining parts seems only few experimental steps away at this point.

9 Acknowledgements

I would like to thank Janos Vörös for giving me the opportunity to work on this project in his Laboratory of Biosensors and Bioelectronics at the Institute for Biomedical Engineering.
A special thank you goes to my supervisor Csaba Forro and my examiner Marta Bally!

I would also like to thank the rest of the team for their support. It was an educational experience.

As always, a big thank you also goes to my family and friends for their solid support.

References

[1] D. Purves, G. J. Augustine, D. Fitzpatrick, W. C. Hall, A.-S. Lamantia, and L. E. White, *Neuroscience*, ch. 1 Studying the Nervous System. Sunderland: Sinauer Associates, fifth ed., 2012.

[2] J. Recknor and S. Mallapragada, *The Biomedical Engineering Handbook: Tissue Engineering and Artificial Organs*, ch. Nerve Regeneration: Tissue Engineering Strategies. New York: Taylor & Francis, third ed., may 2006. J.D. Bronzino, Editor.

[3] J. Roy, T. E. Kennedy, and S. Costantino, "Engineered cell culture substrates for axon guidance studies: moving beyond proof of concept.," *Lab on a chip*, vol. 13, pp. 498–508, feb 2013.

[4] M. D. Boehler, S. S. Leondopulos, B. C. Wheeler, and G. J. Brewer, "Hippocampal networks on reliable patterned substrates.," *Journal of neuroscience methods*, vol. 203, pp. 344–53, jan 2012.

[5] H. Huang, L. Jiang, S. Li, J. Deng, Y. Li, J. Yao, B. Li, and J. Zheng, "Using microfluidic chip to form brain-derived neurotrophic factor concentration gradient for studying neuron axon guidance.," *Biomicrofluidics*, vol. 8, p. 014108, jan 2014.

[6] R. Hu, D. Huang, J. Tong, Q. Liao, Z. Hu, and W. Ouyang, "Aspartic acid in the hippocampus: a biomarker for postoperative cognitive dysfunction," *Neural Regeneration Research*, vol. 9, no. 2, pp. 143–152, 2014.

[7] N. Li and A. Folch, "Integration of topographical and biochemical cues by axons during growth on microfabricated 3-D substrates.," *Experimental cell research*, vol. 311, pp. 307–16, Dec. 2005.

[8] H. Francisco, B. B. Yellen, D. S. Halverson, G. Friedman, and G. Gallo, "Regulation of axon guidance and extension by three-dimensional constraints.," *Biomaterials*, vol. 28, pp. 3398–407, Aug. 2007.

[9] L. Wei, A. J. Sweeney, L. Sheng, Y. Fang, M. S. Kindy, T. Xi, and B. Z. Gao, "Single-neuron axonal pathfinding under geometric guidance: low-dose-methylmercury developmental neurotoxicity test.," *Lab on a chip*, vol. 14, pp. 3564–71, Sept. 2014.

[10] L. Akesso, *GM 1060 SU-8-negative tone photo-epoxy for layers from 6.0 to 50um Technical Datasheet*. Gersteltec Sarl., Générale Guisan 26, 1009 Pully, Switzerland, updated jan. 12th 2005 ed., jan 2005.

[11] T. J. Fellers and M. W. Davidson, "Theory of confocal microscopy - introduction to confocal microscopy." `http://www.olympusfluoview.com/theory/confocalintro.html`. Accessed November 8, 2015.

[12] T. F. S. Inc., "Cell tracking." `https://www.thermofisher.com/de/de/home/life-science/cell-analysis/cell-tracing-tracking-and-morphology/cell-tracking.html`. Accessed January 21, 2016.

[13] S. Mukhopadhyay, "What is transfection? how is it done?." https://www.quora.com/What-is-transfection-How-is-it-done, sep 2013. Accessed November 8, 2015.

[14] micro resist technology, Koepenicker Str. 325, D-12555 Berlin, *processing guidelines - negative tone photoresist series ma-N 1400*.

[15] Gersteltec Sarl., Générale Guisan 26, 1009 Pully, Switzerland, *GM 1075 SU-8-negative tone photo-epoxy for thick layers (>100 um) Technical Datasheet*, updated jun 2007 ed., jan 2015.

[16] J. Monahan, A. a. Gewirth, and R. G. Nuzzo, "A Method for Filling Complex Polymeric Microfluidic Devices and Arrays," *Analytical Chemistry*, vol. 73, pp. 3193–3197, July 2001.

Appendix: CLSM Automatization Protocol

The automated imaging of a sample in the CLSM was conducted according to the following protocol:

1. Heat the cell box to $37°C$ and set the 488nm laser to 'Standby' in the software. Wait until the box is heated.

2. Place the sample in the holder. Pre-align and focus structure in 'Ocular: Online' mode.

3. Switch to 'Acquisition' mode, tick 'Tile Scan' and 'Positions' and set parameters according to your structures. Our microstructures were designed to fit into 2x1 (1800x900μm) tiles. 'Positions: Sample Carrier' was set as depicted in Figure 12.

Figure 12: Screen shot of the 'Sample Carrier' parameters used for our automatized CLSM imaging protocol.

4. Switch to 'Acquisition: Live' mode and move the field of view to one of the microwells in a corner (e.g. microstructure '20-9'). 'Calibrate' 'Sample Carrier' at the respective position (e.g. 'I-1'). You can now move the field of view to any programmed position by clicking the respective square (see Figure 12).

5. This way, check whether the microwells are well within the field of view for all four corners of the sample. If not, manually rotate the sample on the sample holder until they are. You might have to repeat the calibration a couple of times during this process.

6. Once the real sample carrier is thoroughly aligned with the programmed sample carrier, the sample has to be leveled so that all the position are in focus. Therefore, again go to all 4 corners and use the screws at the corners of the sample holder to manually bring all four corners into focus.

7. Adjust other parameters in 'Acquisition Mode', 'Channels', etc. according to the specific requirements of your sample to optimize image quality versus imaging time.

8. Start automatized imaging with 'Start Experiment'.